Methylene blue adsorption onto native watermelon rind: batch and fixed bed column studies

R. Lakshmipathy[a], N.C. Sarada[b],*

[a]Centre for Material Science, KCG College of Technology, Karapakkam, Chennai, Tamilnadu 600097, India, Tel. +91 9994829939; email: lakshmipathy.vit@gmail.com
[b]Environmental and Analytical Chemistry division, School of Advanced Sciences, VIT University, Vellore, Tamilnadu 632014, India, Tel. +91 416 2202359; email: ncsarada@vit.ac.in

ABSTRACT

This study reports the feasibility of waste watermelon rind as adsorbent for the removal of methylene blue in batch and continuous column studies. Batch mode adsorption studies were performed by varying the batch parameters such as pH, contact time, adsorbent dose, initial dye concentration, and temperature. The equilibrium data were analyzed with Langmuir, Freundlich, and Temkin isotherm models and found to better with Langmuir and Temkin models. The kinetic data reveal that the present system follows pseudo-second-order kinetic model. Thermodynamic studies reveal that the present process is spontaneous and exothermic in nature. Fixed bed column studies were performed by varying the column parameters such as flow rate, bed height, and initial inlet concentration. The breakthrough curves obtained were analyzed with Adams–Bohart, Thomas, and Yoon–Nelson models. The results show that watermelon rind an agro waste can be successfully employed for the elimination of methylene blue from aqueous solution.

Keywords: Watermelon rind; Methylene blue; Adsorption; Fixed bed

1. Introduction

Synthetic dyes are widely used in textile, leather, paper, food, pigments, plastics, and cosmetic industries to color the final products. Rapid industrialization has resulted in increased disposal of colored water into the aquatic environment. Discharge of colored dye effluents into natural resources has caused many problems like carcinogenicity, skin allergy, and irritation [1,2]. In view of the toxicity, a lot of techniques such as photodegradation, chemical coagulation, trickling filter, and activated sludge are developed for treatment of colored water. In practical, these techniques are found to be less adaptable and expensive [3]. It is now well established that for the wastewater treatment, adsorption has several advantages such as cost-effective, easy operation, and rapid technique over other methods [4,5]. Moreover, the ability of adsorption to remove toxic chemicals without producing any toxic byproducts, thereby keeping quality of water undisturbed, has also popularized the adsorption technique in comparison with other techniques [6].

Biosorption is the "cost-effective technique" for dye removal. Many low-cost agricultural wastes such as peanut husk [7], rice husk [8], coconut husk [9],

---

*Corresponding author.

rejected tea [10], lotus leaf [11], cotton stalk [12], garlic peel [13], banana peel, and orange peel [14]. Agricultural waste in biosorption system has been drawn greater attention because of abundantly available, cost-effective, ready to use without any pretreatment and regeneration of material may not be necessary unlike activated carbon. However, the use of agricultural waste remains limited due to insufficient documentation for treatment of real-time waste water.

Watermelon (*Citrullus lanatus*), being the largest and heaviest fruit, is one of the most abundant and cheap fruits available in India. Watermelon production occupies 6–7% of overall fruit production and is high during summer because of its tropical nature. Watermelon rind is a by-product from watermelon, which consists of many constituents like proteins, pectin, cetrulline, and caroteniods [15–17]. Due to the presence of hydroxyl, carbonyl, and carboxyl groups watermelon rind is known to bind cations from aqueous solution [18,19]. This study was aimed at the removal of methylene blue, a cationic dye, from aqueous solution by watermelon rind. Batch parameters such as pH, adsorbent dose, contact time, initial dye concentration, and temperature were investigated. Various isotherms and kinetic models were employed to study the adsorption process. Further, adsorption of MB in fixed bed column was investigated to access the practical utility of the watermelon rind.

2. Materials and methods

2.1. Preparation of adsorbent

Watermelon rinds (WR) was obtained from local fruit market and washed under tap water several times followed by double-distilled water. After thorough washing, WR was cut in to small pieces and dried under sun light for 7 d to remove all moisture content present. Later, the dried WR pieces were washed with hot water (70°C) to remove any soluble matter present and dried in oven at 85°C for 48 h. The oven dried WR was powdered using conventional mixture and sieved through 100 BSS mesh. The sieved WR powder was stored in desiccators and used for batch experiments. For fixed bed column studies, WR sieved between 100 and 500 BSS mesh range were employed. The adsorption experiments were carried without any pretreatment of WR.

2.2. Preparation of dye solution

The 1,000 mg L^{-1} stock solution was prepared by dissolving 1 g of MB in 1 L of deionized water. pH adjustments were done using 0.1 M HCl and 0.1 M NaOH solutions. All reagents were of AR grade and deionised water was used for dilutions. The chemical structures and general data of MB are represented in Fig. 1 and Table 1.

2.3. Batch mode adsorption studies

The adsorption of MB on to WR was investigated in batch mode adsorption equilibrium methods. All batch experiments were carried in 100 mL conical flasks containing 20 mL of MB solutions. Sorption capacity of WR was determined by contacting 0.5 g L^{-1} of sorbent with 20 mL of known concentrations (50–300 ppm) of MB solutions at room temperature. The solid phase was separated by centrifugation at 5,000 rpm for 10 min and the residual concentration of supernatant solution was determined by UV–visible spectrophotometer. The effect of pH on adsorption capacity of WR was evaluated in the range of pH 2–10, initial pH of each MB solution was adjusted to desired value using 0.1 M HCl or 0.1 M NaOH. The effect of solid phase on adsorption was studied by varying the dose between 0.5 and 5 g L^{-1} and rate of MB sorption was determined by analyzing the residual concentration of MB ions at different time intervals (10–120 min). All the experiments were conducted in triplicates and average values are reported in this study. The relative standard deviation was found to be not more than 4% for the results. The amount of
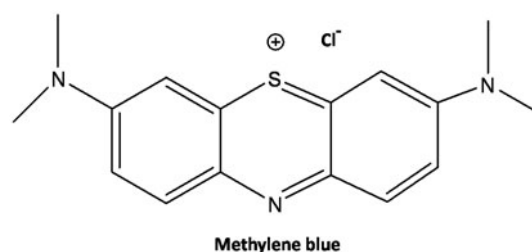

Fig. 1. Structure of methylene blue.

Table 1
General data of methylene blue

Parameter	Values
CI No	52,015
Mol wt	373.88
λ_{max} (nm)	668
Width (nm)	1.43
Depth (nm)	0.61
Thickness (nm)	0.4

MB adsorbed to WR was determined by Eq. (1) and % removal was evaluated by Eq. (2).

$$q_e = (C_0 - C_1)\frac{v}{m} \qquad (1)$$

$$\% \text{ Removal} = \frac{(C_0 - C_1)}{C_0} \times 100 \qquad (2)$$

where q_e is the dye uptake (mg g^{-1}) by WR, C_0 and C_1 are initial and final concentrations of MB (mg L^{-1}), V is the solution volume (L), and M is the mass of the adsorbent (g).

2.4. Column adsorption studies

Continuous column adsorption experiments were performed in laboratory glass column with an internal diameter of 1 cm and a length of 15 cm. Initially, the column was packed with WR (0.354 g cm^{-1}) and synthetic MB solution was fed into the column from upwards at a desired flow rate using a peristaltic pump. The samples were collected at exit of the column at different time intervals and concentration of the eluted samples was determined by measuring the absorbance in UV–visible spectrophotometer. To study the effect of flow rate on adsorption of MB onto WR, experiments were conducted at three different flow rates 1, 2, and 3 mL min^{-1}. The effect of bed height on column adsorption process was conducted at three different bed heights 1, 3, and 5 cm keeping other parameters constant. After optimizing the flow rate and bed height, effect of initial concentration of dye was studied at 500, 750, and 1,000 mg L^{-1}. The flow to the column was continued until there was no adsorption i.e., the MB concentration of influent and effluent remained unchanged [20].

2.5. Column data analysis

The performance of packed bed column studies are obtained in the form of breakthrough curves. The time for the breakthrough and shape of the curve are very important characteristics for determining the operation and dynamic response of a sorption column [21]. The breakthrough point of S-shaped curve is considered when the effluent concentration (C_t) from the column reaches about 0.1% of influent concentration. The column is considered to be saturated or exhausted when the point of concentration of effluent reaches 95%. The breakthrough curve is generally expressed by C_t/C_0 as a function of time or volume of the effluent. The effluent volume can be calculated from the equation as follows:

$$V_{eff} = Qt_{total} \qquad (3)$$

where Q is the volumetric flow rate and t_{total} is the total flow time (min).

The total dye adsorbed, D_{ad} (mg), in the fixed bed column can be calculated from the area under the curve multiplied by the flow rate Eq. (4).

$$D_{ad} = \frac{Q}{1,000} \int_{t=0}^{t=total} C_{ad}\, dt \qquad (4)$$

where C_{ad} is the concentration of dye removal (mg L^{-1}).

The total amount of dye entering the column is (D_{total}) is calculated from the following equation:

$$D_{total} = \frac{C_0 Q t_{total}}{1,000} \qquad (5)$$

And the total dye removal percentage can be obtained from Eq. (6) as follows:

$$Y\ (\%) = \frac{D_{ad}}{D_{total}} \times 100 \qquad (6)$$

3. Results and discussion

3.1. Characterization of adsorbent

The WR was characterized for its physiochemical properties, and the results are summarized in Table 2. FTIR (Avatar 330, Thermo Nicolet, USA) analysis was carried out for WR in order to identify the surface functional groups present for binding MB ions. The FTIR spectra of WR displayed a number of peaks at various wavenumbers pertaining to different functional groups (Fig. 2). The broad and intense peak around 3,378 cm^{-1}

Table 2
Physicochemical characteristics of native watermelon rind

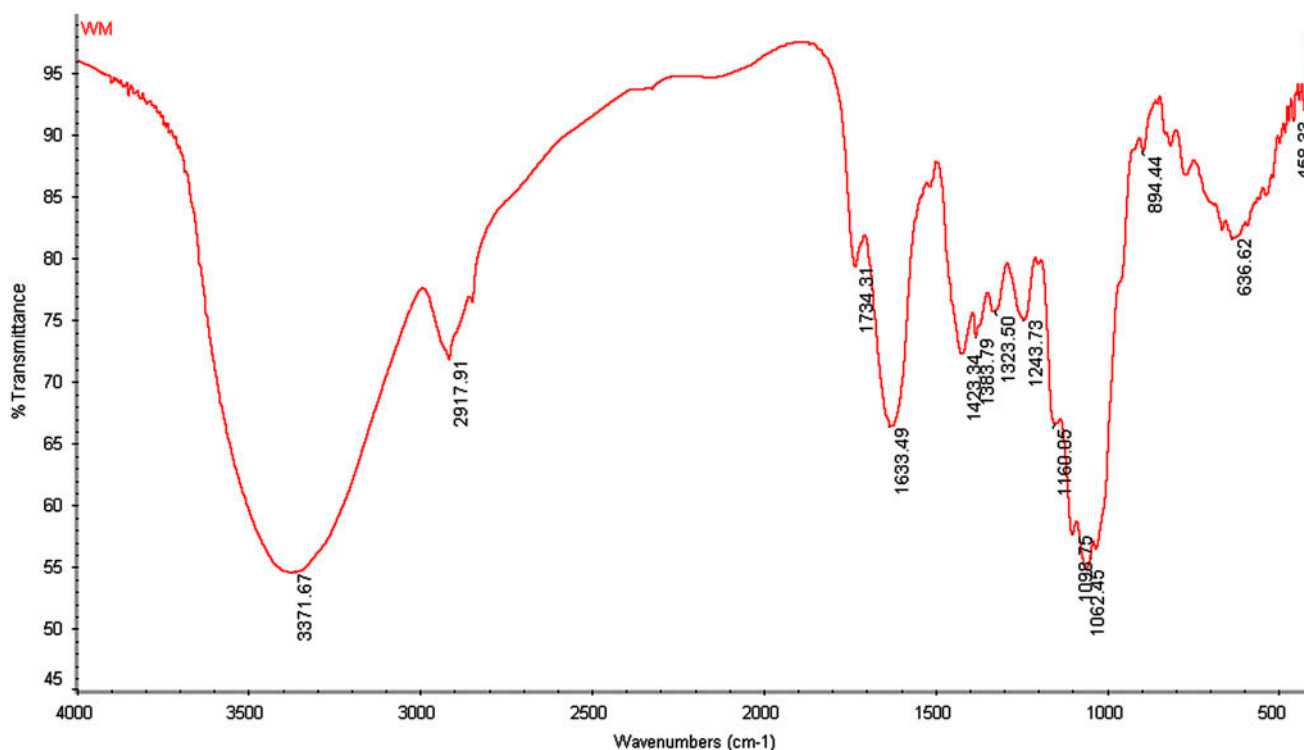| Parameter	WR
Moisture	13%
Particle size	≈74 µm
Density	0.356 g/cc
Carbon	61.47%
Oxygen	30.31%
Total cation content	2.102 meq g^{-1}
pH$_{pzc}$	5.1
Acidic sites	2.51 mmol g^{-1}
Basic sites	0.71 mmol g^{-1}

Fig. 2. FTIR spectra of native watermelon rind.

corresponds to –OH stretching vibrations of cellulose, pectin, and lignin. The peak at 2,917 cm^{-1} attributes to –CH stretching vibrations of methyl and methoxy groups. The peak at 1,728 cm^{-1} corresponds to –C=O stretching of carboxylic acid or esters and asymmetric and symmetric vibrations of ionic carboxylic groups (–COO$^-$), respectively, appeared at 1,621, and 1,421 cm^{-1}. The peak at 1,383 cm^{-1} is assigned to symmetric stretching of –COO$^-$ of pectin. The peaks from 1,350 to 1,000 cm^{-1} can be assigned to stretching vibrations of carboxylic acids and alcohols. It is well indicated from FTIR spectrum of WR that carboxylic and hydroxyl groups are abundantly present and as biopolymers these groups act as proton donors for binding cations.

The surface morphology of WR was studied with scanning electron microscope (XL30 Phillips, Netherland). The SEM image of WR is shown in Fig. 3. It can be observed from the Fig. 3 that the surface of WR is porous like honeycomb structure.

3.2. Batch adsorption studies

3.2.1. Effect of pH on adsorption

One of the important parameters considered during the adsorption process is pH, due to competitive
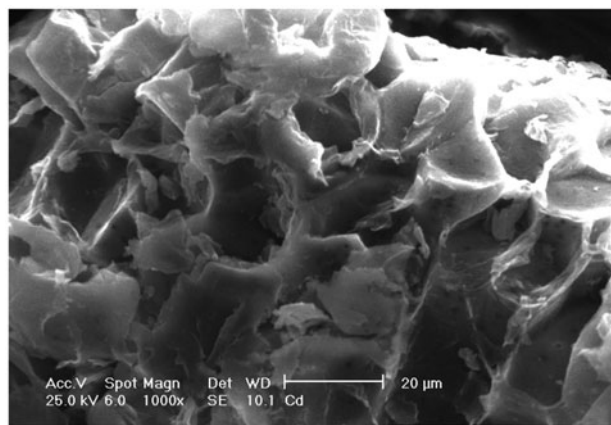

Fig. 3. SEM image of native watermelon rind.

adsorption for active sites by H$^+$ ions. The FTIR spectroscopic analysis show that the WR has variety of functional groups such as carbonyl, carboxyl, and hydroxyl groups which are involved in almost all the potential binding mechanism. Moreover, depending on the solution pH, the functional groups precipitate in cation bindings. The effect of pH was studied by varying the pH in the range of 2–10 for MB (Fig. 4). It was observed that pH has no effect on adsorption of
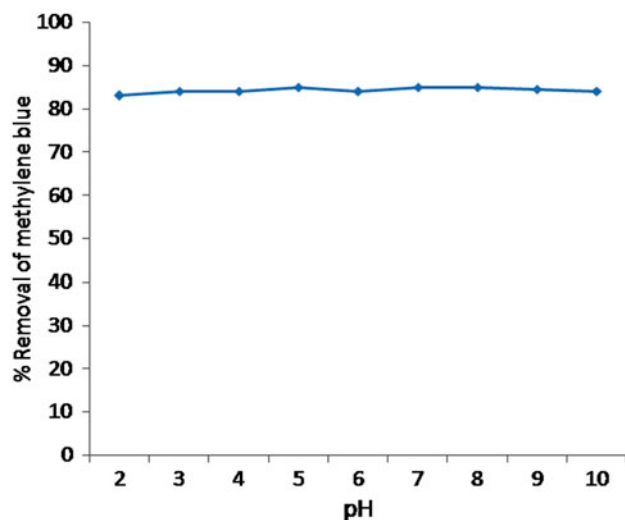
Fig. 4. Plot of effect of pH on the removal of MB ions from aqueous solution by WR (time 30 min, dose 1 g L^{-1}, initial MB concentration 50 mg L^{-1}, and temperature 303 K).

MB onto WR between pH 2–10. This can be attributed to that the electrostatic attraction is not the only mechanism for the removal of WR some other mechanism might be operating for binding. On the other aspect, the presence of more number of active sites on the surface of WR might have minimized the competitive adsorption between H$^+$ and MB ions resulting in nil effect of pH at low initial concentrations. Hence, further experiments were carried out at pH 7.

3.2.2. Effect of salt ionic strength

It is important to discuss the effect of salt ionic strength on the adsorption of MB onto WR. Industrial dyeing effluents usually contain high salt concentration. In order to study the adsorption capability of WR toward cationic dyes in presence of ionic salts, salts such as NaCl, CaCl$_2$, and KCl with different ionic strength were used to stimulate the salt ionic in water. The results of the study are summarized in Table 3. It is evidenced from Table 3 that the presence of ionic salts in the solution has greatly influenced the sorption capacity of WR. Substantial decrease in sorption capacity was noticed with increase in salt ionic strength from 0.1 to 0.2 mol L^{-1}. Since KCl, NaCl, and CaCl$_2$ can release K$^+$, Na$^+$, and Ca^{2+} ions in solution, these ions may compete with MB for the adsorbent active sites which results in decrease in sorption capacity of WR. It was also observed that further increase in salt strength from 0.2 to 0.3 mol L^{-1} has shown no significant effect on loading capacity of WR. This can be attributed to saturation of electrostatic

Table 3
Effect of ionic salt strength on adsorption of methylene blue by WR (pH 7, time 30 min, initial concentration 50 mg L^{-1}, dose 0.5 g L^{-1}, temperature 303 K)

Salt strength (mol L^{-1})	Salt	Loading capacity (q_e mg g^{-1})
0	–	44.5
0.1	KCl	29.6
	NaCl	30.5
	CaCl$_2$	28.6
0.2	KCl	16.6
	NaCl	16.9
	CaCl$_2$	16.3
0.3	KCl	15.4
	NaCl	15.9
	CaCl$_2$	15.2

attractive active sites and rest of the adsorption of MB onto WR must be governed by some other mechanism.

3.2.3. Desorption studies

Desorption and regeneration studies were performed to know the reusability potential of WR. Desorption of dyes from WR were studied by using 0.1 M HCl, 0.1 M acetic acid, distilled water, and 0.1 M NaOH as desorbing agents. It was observed that 0.1 M acetic acid and 0.1 M HCl showed highest desorption percentage compared to NaOH and water (Fig. 5). The order was found to be Acetic acid > HCl > NaOH > Water. However, the maximum desorption
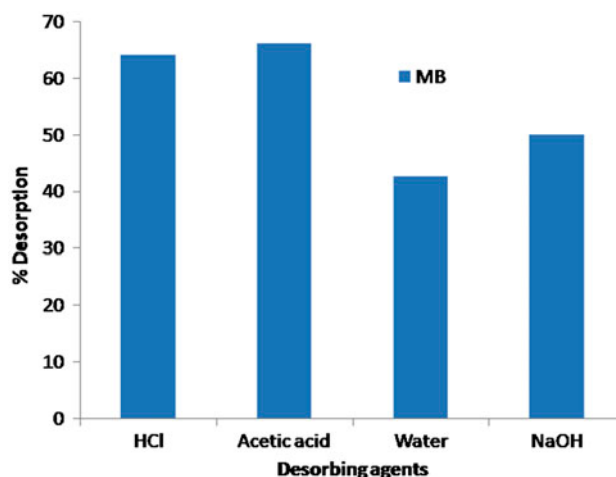

Fig. 5. Plots of desorption of MB ions from WR with different desorbing agents (time 30 min, dose 1 g L^{-1} of 47.5 mg g^{-1} MB loaded WR, and temperature 303 K).

percentage attained from WR with acetic acid was found to be only 66% for MB. The moderate desorption percentage observed might be due to aromatic–aromatic interaction of MB with WR. These observations suggest that WR can be used for single cycle to remove cationic dyes from aqueous solution effectively.

3.3. Kinetics of adsorption

The equilibrium kinetic data obtained for the removal of MB by WR are represented in Fig. 6. To analyze the mechanism and rate of adsorption of dyes onto WR, experimental data obtained were fitted to Lagergren's pseudo-first-order and pseudo-second-order models.

The Lagergren's rate equation is one of the most widely used rate equation for study of adsorption of an adsorbate from aqueous solution. The linear form of Lagergren's pseudo-first-order equation is given as follows:

$$\ln (q_e - q_t) = \ln q_e - k_1 t \tag{7}$$

where q_e is the amount of metal adsorbed at equilibrium (mg g^{-1}), q_t is the amount of metal adsorbed at time t, and k_1 is the first-order reaction rate constant. The values of k_1 and q_e can be determined from the slopes and intercepts of $\ln (q_e - q_t)$ vs. t plots.

The pseudo-second-order kinetic model is the other most widely used model and the expression used in this study is as follows:
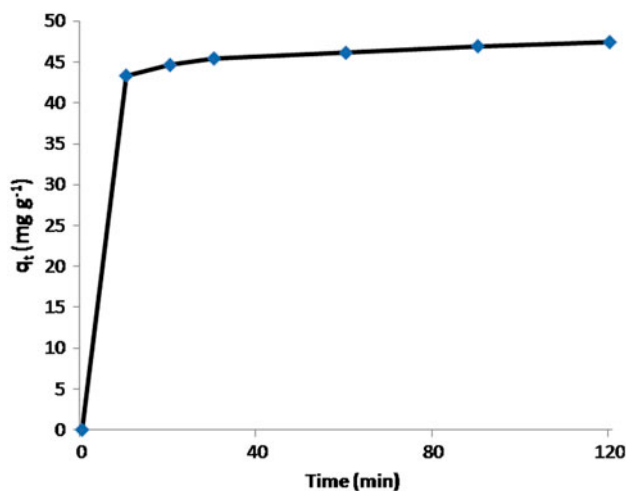

Fig. 6. Kinetic plot for the removal of MB ions from aqueous solution by WR.

$$\frac{t}{q_t} = \frac{1}{k_2 q_e^2} + \frac{t}{q_e} \tag{8}$$

where k_2 (g mg^{-1} min^{-1}) is the rate constant of pseudo-second-order adsorption. The values of k_2 and q_e can be determined from the plots of t/q_t vs. t.

The respective parameters of pseudo-first-order and pseudo-second-order models are represented in Table 4. The low correlation coefficients and low q_e values obtained for pseudo-first-order model suggest that the removal of MB by WR does not follow pseudo-first order. The pseudo-second-order model resulted in a straight and the correlation coefficients obtained was close to one. The theoretical q_e values obtained are close to the calculated experimental values which show the appropriateness to the model. These observations suggest that the removal of dyes onto WR follows pseudo-second-order kinetic model. According to pseudo-second order, boundary layer resistance is not the rate-limiting step, the external resistance model cannot adequately describe the adsorption mechanism, and the process controlling the rate may be a chemical sorption involving valences forces through sharing or exchanging of electrons between sorbate and sorbent.

Kinetic data were further analyzed using intraparticle diffusion model in order to study the steps of diffusion mechanisms.

$$q_t = k_{int} t^{\frac{1}{2}} + C \tag{9}$$

A plot of q_t vs. $t^{1/2}$ should result in straight line if the adsorption mechanism follows intraparticle diffusion process only. If the plot shows multi-linear plots, it indicates that two or more steps take place. The plot of present process resulted in multi-linear plot for WR (Fig. 7). The first linear plot of MB for WR is due to the immediate utilization of ample active sites on the

Table 4
Kinetic parameters of MB removal by WR from aqueous solution (pH 7, dose 1 g L^{-1}, initial concentration 50 mg L^{-1}, and temperature 303 K)

Model	Parameters	MB
Experimental	q_e (mg g^{-1})	44.5
Pseudo-first order	q_e (mg g^{-1})	1.26
	k_1 (min^{-1})	0.021
	R^2	0.980
Pseudo-second order	q_e (mg g^{-1})	43.6
	k_2 (g mg^{-1} min^{-1})	0.036
	R^2	0.999
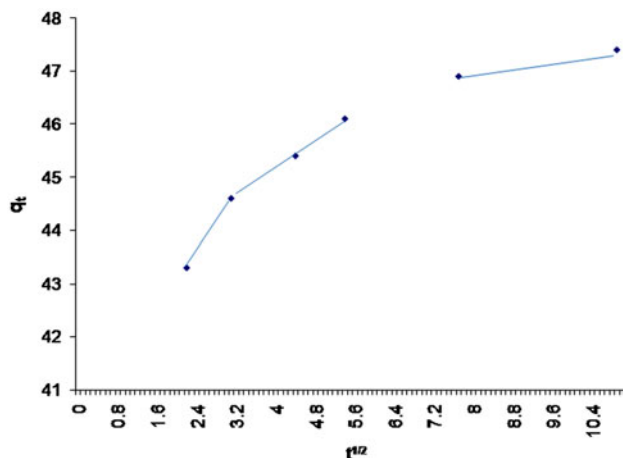
Fig. 7. Weber and Morris intraparticle diffusion plot for the removal of MB ions from aqueous solution by WR.

Fig. 8. Adsorption equilibrium plot for the removal of MB ions from aqueous solution by WR.

adsorbent surface and the second and third linear plots are attributed to very slow diffusion of the adsorbate from the surface site into the inner pores [22]. Thus, initial adsorption of MG by WR may be governed by intraparticle transport of surface diffusion and the later part may be controlled by pore diffusion [23]. However, the intercept of the line for all the studied dyes fails to pass through the origin which may attribute to the difference in the rate of mass transfer in the initial and final stages of adsorption [24].

3.4. Adsorption isotherms

The adsorption equilibrium data obtained for the removal of MB ions at different initial dye concentrations by WR are represented in Fig. 8. In order to examine the relationship between concentration of dye at equilibrium (C_e) and loading capacity (q_e) equilibrium data were analyzed with Freundlich, Langmuir, and Temkin isotherm models.

The linear form of Freundlich isotherm is given as

$$\log q_e = \log k_f + \frac{1}{n} \log C_e \tag{10}$$

where k_f and n are Freundlich constants indicating adsorption capacity and intensity, respectively. If Eq. (10) applies, a plot of log q_e vs. log C_e will give a straight. The linear form of Langmuir equation after rearrangement is given as

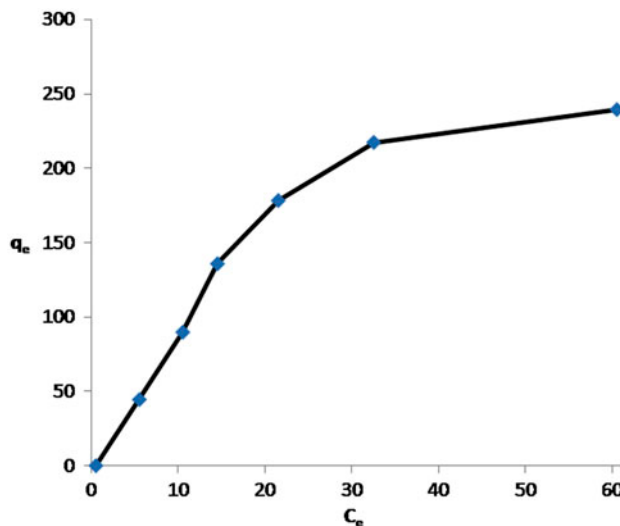$$\frac{C_e}{q_e} = \frac{1}{bV_m} + \frac{C_e}{V_m} \tag{11}$$

where BR is the concentration of solution at equilibrium (mg^{-1}), q_e is the amount of dye adsorbed per mass unit of adsorbent (mg g^{-1}), V_m is the amount of adsorbate at complete monolayer coverage (mg g^{-1}), and b is a constant that relates to the heat of adsorption (L mg^{-1}). If the biosorption follows Langmuir isotherm, then a plot of C_e/q_e should be a straight line with slope $1/V_m$ and intercept $1/bV_m$.

The Temkin isotherm considers the effect of the adsorbate interaction on adsorption at active sites. The linear form of equation is given as

$$q_e = B \ln A + B \ln C_e \tag{12}$$

where A is the equilibrium binding constant (L/mg) and B is related to the heat of adsorption. A plot of q_e vs. ln C_e enables the determination of isotherm constants.

The correlation coefficients and respective constants obtained for Freundlich, Langmuir, and Temkin isotherms are summarized in Table 5. The low correlation coefficient obtained for Freundlich isotherm suggests that this model might not be applicable to the present system. The correlation coefficients obtained for Langmuir and Temkin isotherm were close to one suggesting better fit to the equilibrium data. The better fit to Langmuir isotherm was further supported by theoretical monolayer coverage (V_m). The theoretical monolayer coverage (V_m) of MB onto WR was found to be 232.2 mg g^{-1} against 239.7 mg g^{-1} found experimentally. The loading capacity of WR toward MB was

Table 5
Isothermal parameters derived for the removal of MB by WR from aqueous solution (pH 7, time 30 min, dose 1 g L^{-1}, and temperature 303 K)

Isotherm	Parameter	MB
Freundlich	k_f	7.41
	$1/n$	0.06
	R^2	0.870
Langmuir	q_{max} (mg g^{-1})	243.9
	b (L mg^{-1})	0.04
	R^2	0.963
Temkin	A	16.25
	B	4.58
	R^2	0.956

found to be higher than many other adsorbents reported in literature.

3.5. Thermodynamics of adsorption

In order to describe the thermodynamic behavior of sorption of MB onto WR at equilibrium, temperature was varied from 303 to 323 K. It was observed that with increase in temperature, the adsorption capacity of WR increased from 44.5 to 46.1 mg g^{-1}. The observed increase in capacity might be due to increase in the diffusion rate of MB ions in to the pores of WR at high temperatures. Thermodynamic parameters including change in free energy ($\Delta G°$), enthalpy ($\Delta H°$), and entropy ($\Delta S°$) were derived from the following equations:

$$K_D = \frac{q_e}{C_e} \tag{13}$$

$$\Delta G° = -RT \ln K_D \tag{14}$$

$$\Delta G° = -\Delta H° - T\Delta S° \tag{15}$$

where K_D is the equilibrium constant related to the Langmuir constant "b", R is the universal gas constant (8.314 J Mol^{-1} K^{-1}), and T is temperature in Kelvin.

The thermodynamic parameters calculated for the removal of MB by WR from aqueous solution are represented in Table 6. The change in free energy $\Delta G°$ was found to be negative and the negative values were found to increase with increase in temperature which shows that the system is more spontaneous at higher temperature. The negative $\Delta H°$ values indicate the process is exothermic in nature and positive $\Delta S°$ values indicate the increase in the randomness of solid–liquid interface during the adsorption.

3.6. Column studies

3.6.1. Effect of flow rate

Flow rate of influent in fixed bed adsorption process is one of the important parameters to be studied. The breakthrough curves obtained for different flow rates of influent solution is shown in Fig. 9. As the flow rate increased from 1 to 3 mL, the exhaustion time decreased from 115 to 75 min and the total dye removal % also substantially decreased from 71.7 to 21%. The decrease in exhaustion time and removal efficiency can be attributed to decrease in residence time of adsorbate and external mass transfer resistance at the surface of the adsorbent [25]. The dye uptake capacity was also substantially influenced by flow rate. The uptake capacity of WR for MB decreased from 116.5 to 70 mg g^{-1}, respectively, as the flow rate increased from 1 to 3 mL min^{-1} (Table 7). Similar tendency has been found by other researchers for the removal of MB in fixed bed column system [26–28].

3.6.2. Effect of bed height

The breakthrough curves at different bed heights are shown in Fig. 10 and sorption column data are presented in Table 7. With increase in bed height, the exhaustion time and influent volume increased, this is due to more contact time. Similarly, the removal efficiency also increased from 71 to 88% with increase in bed height. The increase in efficiency at higher bed height is due to availability of more number of surface sites and increased volume of influent [20]. Since the

Table 6
Thermodynamic parameters derived for the removal of MB onto WR (pH 7, contact time 30 min, dose 1 g L^{-1}, and initial concentration 50 mg L^{-1})

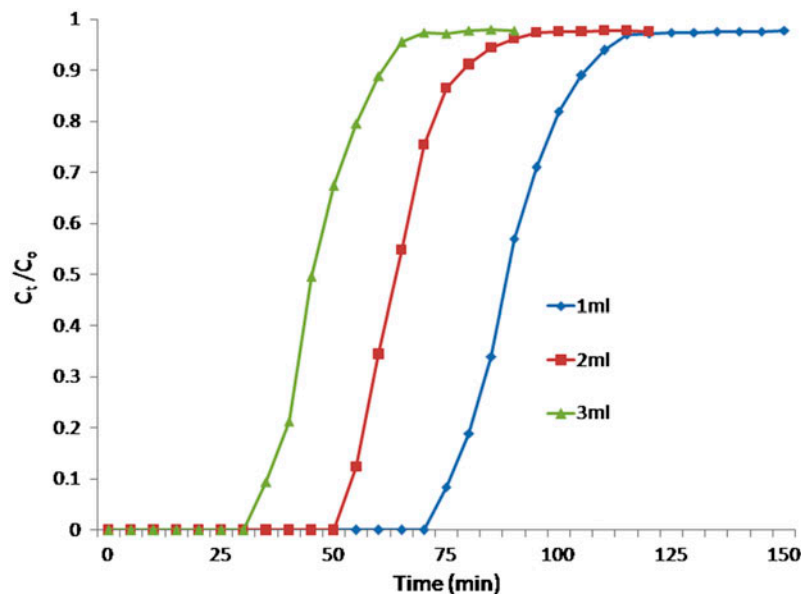| Dye	Temperature (K)	Loading capacity (q_e)	$\Delta G°$ (kJ mol^{-1})	$\Delta H°$ (kJ mol^{-1})	$\Delta S°$ (J mol^{-1} K^{-1})
MB	303	44.5	−5.26	−4.59	670
	313	45.4	−5.93		
	323	46.1	−6.60		

Fig. 9. Breakthrough curves obtained at different flow rates for the removal of MB ions by WR.

Table 7
Parameters in fixed bed column for the removal of MB from aqueous solution by WR

C_0 (mg L^{-1})	Q (mL min^{-1})	Z (cm)	D_{ad} (mg)	D_{total} (mg)	Y (%)	EBCT (min)
500	1	1	41.2	57.5	71.7	3.0
500	2	1	31.4	90	34.8	2.10
500	3	1	24.8	112.5	22.0	1.20
500	1	1	41.2	57.5	71.7	3.0
500	1	3	76.2	90	84.6	9.20
500	1	5	103.7	117.5	88.2	14.55
500	1	5	103.7	117.5	88.2	14.55
750	1	5	124.1	142.5	87.0	14.55
1,000	1	5	125.4	145	82.5	14.55

flow rate is optimized prior to bed height, the lower flow rate facilitates increased residence time for the adsorbates at higher bed depths. With increase in bed height, the empty bed contact time also increased from 3.1, 7.2 to 12.2 min for 1, 3, and 5 cm bed heights, respectively. These results indicated that the bed height of 5 cm offered higher removal efficiency, exhaustion time, and influent volume. Therefore, subsequent experiments were carried out with this bed height.

3.6.3. Effect of MB initial concentration

The breakthrough curves at different initial concentrations of MB are shown in Fig. 11. The breakthrough time and column exhaustion time decreased with increase in initial dye concentration. This can be explained by the fact that at the greater concentration gradient caused a faster transport due to increased diffusion coefficient or mass transfer coefficients [29]. As expected, with increase in initial concentration the loading capacity increased from 63.2 to 78.3 mg g^{-1}. It was observed that the column achieved saturation at 750 mg L^{-1} and beyond which the loading capacity was found to be same. The percentage removal of MB was found to gradually decrease with gradual increase in initial inlet concentration. The breakthrough curves were sharp at high inlet concentrations of MB, implying a relatively smaller mass transfer zone and intra particle diffusion control. Similar observations have been reported by other researchers [20,30].
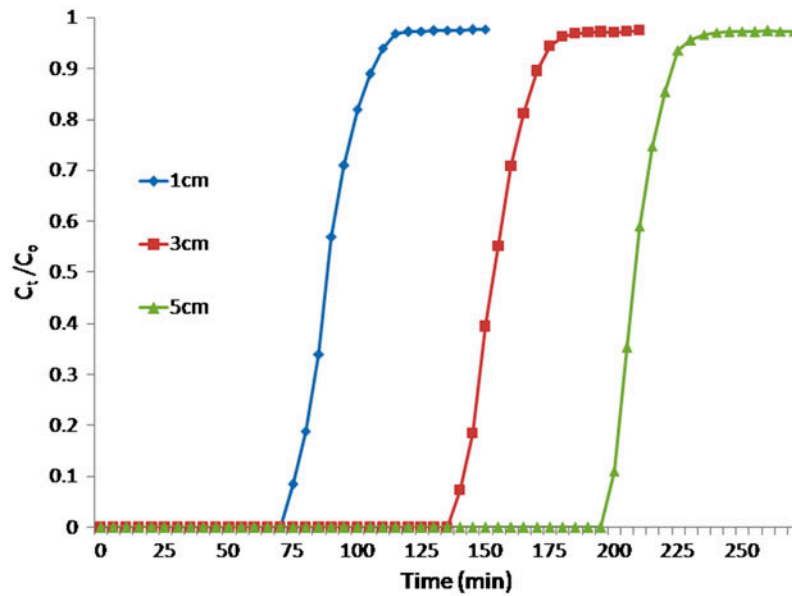
Fig. 10. Breakthrough curves obtained at different bed heights for the removal of MB ions by WR.
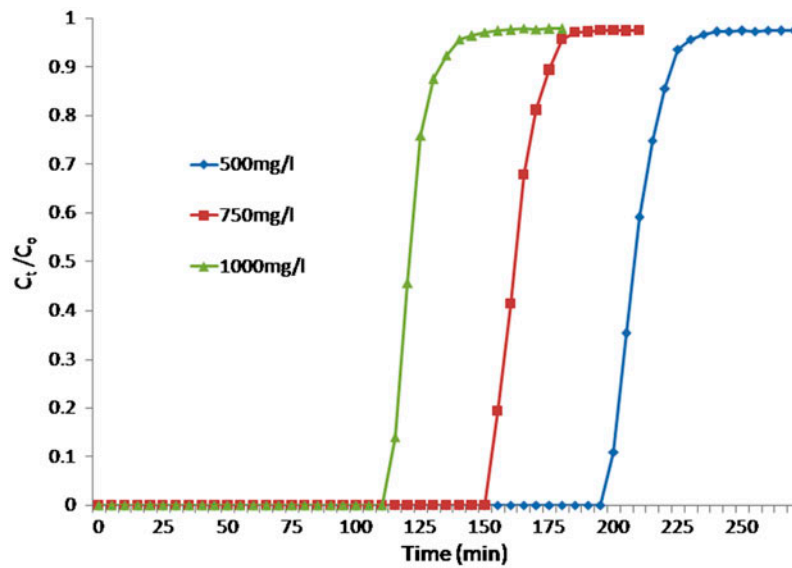

Fig. 11. Breakthrough curves obtained at different initial concentrations for the removal of MB ions by WR.

3.7. Breakthrough curve modeling

The successive operation of laboratory scale column toward industrial applications can be well explained by simple mathematical models [31,32]. The breakthrough curves obtained for flow rate, bed height, and initial dye concentration was predicted with well-known mathematical models such as Adams–Bohart, Thomas, and Yoon–Nelson models.

3.7.1. Adams–Bohart model

Adams–Bohart model is one of the most widely used models for prediction of column breakthrough curves. According to this model, the equilibrium is not instantaneous and the rate of sorption is proportional to the fraction of sorption capacity [33,34]. This model is used to explain the initial part of the breakthrough curve and the model equation is expressed as

$$\ln\frac{C_t}{C_0} = k_{AB}C_0 t - k_{AB}N_0 \frac{z}{U_0} \qquad (16)$$

where C_0 and C_t are the inlet and outlet adsorbate concentrations (mg L^{-1}), k_{AB} is the kinetic constant (L mg^{-1} min^{-1}), N_0 is the saturation concentration (mg L^{-1}), z is the bed height (cm), and U_0 is superficial velocity (cm min^{-1}).

For evaluation of parameters, the range of t taken into consideration was from the beginning to the end of the breakthrough curves. The values of ln (C_t/C_0) were plotted against t and from slope and intercept, k_{AB} and N_0 were calculated. The values of k_{AB} and N_0 for all breakthrough curves are represented in Table 8, along with respective correlation coefficients. The values of k_{AB} increased with increase in flow rate and decreased with increase in bed height and increase in initial concentration. It was indicated that the overall system kinetics was dominated by external mass transfer in the initial part of adsorption in fixed bed column [21,25].

3.7.2. Thomas model

One of the most general and widely used models for describing the performance theory of sorption process in fixed bed column is Thomas model [35]. This model assumes the plug flow behavior in bed and the equation is expressed as

$$\ln\left(\frac{C_0}{C_t} - 1\right) = \frac{k_{Th}q_0 m}{Q} - k_{Th}C_0 t \qquad (17)$$

where k_{Th} is the Thomas model constant (mL min^{-1} g^{-1}) and q_0 is the adsorption capacity (mg g^{-1}). The values of k_{Th} and q_0 can be determined from the slope and intercept of ln (C_0/C_t-1) against t.

The values of k_{Th} and q_0 obtained for all breakthrough curves including correlation coefficients are represented in Table 9. It can be observed from Table 8, the values of k_{Th} increased with increase in flow rate and increase in bed height and decreased with increase in initial concentration while the values of q_0 loading capacity decreased with increase in flow rate and increase in bed height. The values of q_0 increased with increase in initial concentration and found saturated beyond 750 mg L^{-1}. The correlation coefficients obtained for all the breakthrough curves were found to be between 0.937 and 0.993 which depicts the better fit of Thomas model to the present system compared to Adams–Bohart model.

3.7.3. Yoon–Nelson model

Yoon–Nelson [36] developed a relatively simple model for the adsorption of vapors or gasses in activated coal. This model assumes that the rate of decrease in the probability of adsorption for each adsorbate molecule is proportional to the probability of sorbate sorption and the probability of sorbate breakthrough on sorbent. The linear form of the equation is

$$\ln\left(\frac{C_t}{C_0 - C_t}\right) = k_{YN}t - \tau k_{YN} \qquad (18)$$

where k_{YN} is the Yoon–Nelson proportionality constant in min^{-1} and τ is the time required for retaining 50% of the initial sorbate (min). The values of k_{YN} and τ can be determined from slope and intercept of plots $\ln(C_t/C_0–C_t)$ vs. t.

The values of k_{YN} and τ obtained for all breakthrough curves including correlation coefficients are represented in Table 10. It can be observed from

Table 8
Parameters of Adams–Bohart model under different conditions for the removal of MB

Parameter		K_{AB} (L/mg min)	N_0 (mg/L)	R^2
Flow rate	1 mL	7.2×10^{-3}	21,442	0.951
	2 mL	6.1×10^{-3}	27,876	0.944
	3 mL	5.7×10^{-3}	31,860	0.939
Bed height	1 cm	7.2×10^{-3}	21,442	0.951
	3 cm	6.4×10^{-3}	17,603	0.926
	5 cm	6.2×10^{-3}	15,067	0.935
Initial concentration	500 mg L^{-1}	6.2×10^{-3}	15,067	0.935
	750 mg L^{-1}	5.5×10^{-3}	19,508	0.917
	1,000 mg L^{-1}	5.6×10^{-3}	21,579	0.913

Table 9
Parameters of Thomas model at different conditions for the removal of MB

Parameter		K_{TH} (mL/min mg)	q_0 (mg/g)	R^2
Flow rate	1 mL	1.4×10^{-3}	124.4	0.993
	2 mL	1.5×10^{-3}	105.9	0.975
	3 mL	1.7×10^{-3}	96.2	0.992
Bed height	1 cm	1.4×10^{-3}	124.4	0.993
	3 cm	1.5×10^{-3}	113.5	0.993
	5 cm	1.5×10^{-3}	108.6	0.965
Initial concentration	500 mg L^{-1}	1.5×10^{-3}	108.6	0.965
	750 mg L^{-1}	1.2×10^{-3}	87.7	0.990
	1,000 mg L^{-1}	8.6×10^{-4}	76.9	0.937

Table 10
Parameters of Yoon–Nelson model at different conditions for the removal of MB

Parameter		K_{YN} (min^{-1})	τ (min)	R^2
Flow rate	1 mL	0.715	80.1	0.993
	2 mL	0.729	62.6	0.965
	3 mL	0.837	40.3	0.989
Bed height	1 cm	0.715	80.1	0.993
	3 cm	0.719	153.5	0.983
	5 cm	0.768	204.9	0.961
Initial concentration	500 mg L^{-1}	0.768	204.9	0.961
	750 mg L^{-1}	0.823	153.4	0.987
	1,000 mg L^{-1}	0.829	120.2	0.922

Table 10 that the correlation coefficients are found to be between 0.922 and 0.993 which shows the better fit to this model along with Thomas model. The values of k_{YN} were found to increase with increase in flow rate, bed height, and initial concentration. The time necessary to reach for 50% retention, τ was found to significantly decrease with increase in flow rate and increase in initial inlet concentration. This is due to saturation of column attained quickly while the τ values increased with increase in bed height due to slower saturation of column at higher bed heights. Based on the regression coefficient values, Thomas and Yoon–Nelson models can be used to predict the breakthrough curves for application in large-scale industrial treatment processes.

3.8. Plausible mechanism of adsorption

The presence of surface functional groups plays an important role on adsorption of MB ions onto adsorbent. As demonstrated by Boehm titration method and FTIR analysis, WR consists of variety of functional groups such as hydroxyl, carboxyl, carbonyl, and aromatic structures for potential binding of cations. On the other hand, due to cationic properties of MB, the charge is delocalized throughout the chromophoric system and it is probably more localized on the nitrogen. The width, depth, and thickness of MB are equal to 1.43, 0.61, and 0.4 nm, respectively, allows the easy access within the porous structure of WR [37]. Based on the above facts and evidences observed from salt ionic strength and desorption studies, adsorption of MB onto WR might follow electrostatic attraction, hydrogen bonding, and aromatic–aromatic interaction mechanisms. Based on the results of salt ionic strength and desorption studies, 65% of MB adsorption onto WR follows electrostatic attraction and 35% rest might be of hydrogen bonding and aromatic–aromatic interactions. Since the surface of WR is covered with ample functional groups (total acidic and basic sites - 3.22 mmol g^{-1}), electrostatic attraction mechanism is dominated for MB adsorption.

4. Conclusion

Watermelon rind an agro waste was employed as adsorbent for the removal of methylene blue from aqueous solution by batch and continuous process. Batch results revealed that pH has no effect on adsorption of MB by WR. The kinetic data were well explained by pseudo-second-order model and intraparticle diffusion models shows the removal of MB is multistep processes. The equilibrium data tend to fit well to Langmuir and Temkin isotherm models. Thermodynamics of adsorption revealed the system is spontaneous and exothermic in nature. Fixed bed column studies were performed by varying the flow rate, bed heights, and initial inlet concentration. The % removal decreased with increase in flow rate and increased with increase in bed height. The % removal of MB was found to increase with increase in inlet concentration and decreased beyond 750 mg L^{-1}. Adams–Bohart, Thomas, and Yoon–Nelson models were applied to the experimental data and found that Thomas and Yoon–Nelson models have better fit compared to Adams–Bohart model. These results conclude that native watermelon rind without any pretreatment can be employed as potential adsorbent for removal of MB from aqueous solution.

References

[1] E. Forgacs, T. Cserháti, G. Oros, Removal of synthetic dyes from wastewaters: A review, Environ. Int. 30 (2004) 953–971.

[2] H.S. Rai, M.S. Bhattacharyya, J. Singh, T.K. Bansal, P. Vats, U.C. Banerjee, Removal of dyes from the effluent of textile and dyestuff manufacturing industry: A review of emerging techniques with reference to biological treatment, Crit. Rev. Env. Sci. Technol. 35 (2005) 219–238.

[3] A. Mittal, D. Jhare, J. Mittal, Adsorption of hazardous dye eosin yellow from aqueous solution onto waste material de-oiled soya: Isotherm, kinetics and bulk removal, J. Mol. Liq. 179 (2013) 133–140.

[4] V.K. Gupta, Suhas, Application of low-cost adsorbents for dye removal—A review, J. Environ. Manage. 90 (2009) 2313–2342.

[5] A. Demirbas, Agricultural based activated carbons for the removal of dyes from aqueous solutions: A review, J. Hazard. Mater. 167 (2009) 1–9.

[6] A. Srinivasan, T. Viraraghavan, Decolorization of dye wastewaters by biosorbents: A review, J. Environ. Manage. 91 (2010) 1915–1929.

[7] J.Y. Song, W.H. Zou, Y.Y. Bian, F.Y. Su, R.P. Han, Adsorption characteristics of methylene blue by peanut husk in batch and column modes, Desalination 265 (2011) 119–125.

[8] R.P. Han, D.D. Ding, Y.F. Xu, W.H. Zou, Y.F. Wang, Y.F. Li, L.N. Zou, Use of rice husk for the adsorption of congo red from aqueous solution in column mode, Bioresour. Technol. 99 (2008) 2938–2946.

[9] A. Mittal, R. Jain, J. Mittal, M. Shrivastava, Adsorptive removal of hazardous dye Quinoline yellow from wastewater using coconut-husk as potential adsorbent, Fresenius Environ. Bull. 19 (2010) 1–9.

[10] N. Nasuha, B.H. Hameed, Adsorption of methylene blue from aqueous solution onto NaOH-modified rejected tea, Chem. Eng. J. 166 (2011) 783–786.

[11] X. Han, W. Wang, X. Ma, Adsorption characteristics of methylene blue onto low cost biomass material lotus leaf, Chem. Eng. J. 171 (2011) 1–8.

[12] H. Deng, J. Lu, G. Li, G. Zhang, X. Wang, Adsorption of methylene blue on adsorbent materials produced from cotton stalk, Chem. Eng. J. 172 (2011) 326–334.

[13] B.H. Hameed, A.A. Ahmad, Batch adsorption of methylene blue from aqueous solution by garlic peel, an agricultural waste biomass, J. Hazard. Mater. 164 (2009) 870–875.

[14] G. Annadurai, R.S. Juang, D.J. Lee, Use of cellulose-based wastes for adsorption of dyes from aqueous solutions, J. Hazard. Mater. 92 (2002) 263–274.

[15] G.K. Jayaprakasha, K.N.C. Murthy, B.S. Patil, Rapid HPLC-UV method for quantification of l-citrulline in watermelon and its potential role on smooth muscle relaxation markers, Food Chem. 127 (2011) 240–248.

[16] R.M. Rimando, P.M. Perkins-Veazie, Determination of citrulline in watermelon rind, J. Chromatogr. A 1078 (2005) 196–200.

[17] A. Mort, Y. Zheng, F. Qiu, M. Nimtz, G. Bell-Eunice, Structure of xylogalacturonan fragments from watermelon cell-wall pectin. Endopolygalacturonase can accommodate a xylosyl residue on the galacturonic acid just following the hydrolysis site, Carbohydr. Res. 343 (2008) 1212–1221.

[18] R. Lakshmipathy, A.V. Vinod, N.C. Sarada, Watermelon rind as biosorbent for removal of Cd^{2+} from aqueous solution: FTIR, EDX, and Kinetic studies, J. Indian Chem. Soc. 90 (2013) 1147–1154.

[19] R. Lakshmipathy, N.C. Sarada, Application of watermelon rind as sorbent for removal of nickel and cobalt from aqueous solution, Int. J. Miner. Process. 122 (2013) 63–65.

[20] S.S. Baral, N. Das, T.S. Ramulu, S.K. Sahoo, S.N. Das, G.R. Chaudhury, Removal of Cr(VI) by thermally activated weed *Salvinia cucullata* in a fixed-bed column, J. Hazard. Mater. 161 (2009) 1427–1435.

[21] A.A. Ahmad, B.H. Hameed, Fixed-bed adsorption of reactive azo dye onto granular activated carbon prepared from waste, J. Hazard. Mater. 175 (2010) 298–303.

[22] A. Bhatnagar, A.K. Minocha, M. Sillanpää, Adsorptive removal of cobalt from aqueous solution by utilizing lemon peel as biosorbent, Biochem. Eng. J. 48 (2010) 181–186.

[23] E. Kumar, A. Bhatnagar, J.A. Choi, U. Kumar, B. Min, Y. Kim, H. Song, K.J. Paeng, Y.M. Jung, R.A.I. Abou-Shanab, B.H. Jeon, Perchlorate removal from aqueous solutions by granular ferric hydroxide (GFH), Chem. Eng. J. 159 (2010) 84–90.

[24] K.K. Panday, G. Prasad, V.N. Singh, Mixed adsorbents for Cu(II) removal from aqueous solutions, Environ. Technol. Lett. 7 (1986) 547–554.

[25] R.P. Han, L.N. Zou, X. Zhao, Y.F. Xu, F. Xu, Y.L. Li, Y. Wang, Characterization and properties of iron oxide-coated zeolite as adsorbent for removal of

copper(II) from solution in fixed bed column, Chem. Eng. J. 149 (2009) 123–131.

[26] R. Han, Y. Wang, X. Zhao, Y. Wang, F. Xie, J. Cheng, M. Tang, Adsorption of methylene blue by phoenix tree leaf powder in a fixed-bed column: Experiments and prediction of breakthrough curves, Desalination 245 (2009) 284–297.

[27] M. Auta, B.H. Hameed, Chitosan–clay composite as highly effective and low-cost adsorbent for batch and fixed-bed adsorption of methylene blue, Chem. Eng. J. 237 (2014) 352–361.

[28] W. Zhang, L. Dong, H. Yan, H. Li, Z. Jiang, X. Kan, H. Yang, A. Li, R. Cheng, Removal of methylene blue from aqueous solutions by straw based adsorbent in a fixed-bed column, Chem. Eng. J. 173 (2011) 429–436.

[29] Md.T. Uddin, Md. Rukanuzzaman, Md.M.R. Khan, Md.A. Islam, Adsorption of methylene blue from aqueous solution by jackfruit (*Artocarpus heteropyllus*) leaf powder: A fixed-bed column study, J. Environ. Manage. 90 (2009) 3443–3450.

[30] K.S. Rao, S. Anand, P. Venkateswarlu, Modeling the kinetics of Cd(II) adsorption on *Syzygium cumini L* leaf powder in a fixed bed mini column, J. Ind. Eng. Chem. 17 (2011) 174–181.

[31] P.A. Kumar, S. Chakraborty, Fixed-bed column study for hexavalent chromium removal and recovery by short-chain polyaniline synthesized on jute fiber, J. Hazard. Mater. 162 (2009) 1086–1098.

[32] V. Vinodhini, N. Das, Packed bed column studies on Cr(VI) removal from tannery wastewater by neem sawdust, Desalination 264 (2010) 9–14.

[33] W.W. Eckenfelder Jr., Industrial Water Pollution Control, McGraw Hill, New York, NY, 1989.

[34] M. Lehmann, A.I. Zouboulis, K.A. Matis, Modelling the sorption of metals from aqueous solutions on goethite fixed-beds, Environ. Pollut. 113 (2001) 121–128.

[35] H.C. Thomas, Heterogeneous ion exchange in a flowing system, J. Am. Chem. Soc. 66 (1944) 1466–1664.

[36] Y.H. Yoon, J.H. Nelson, Application of gas adsorption kinetics I. A theoretical model for respirator cartridge service life, Am. Ind. Hyg. Assoc. J. 45 (1984) 509–516.

[37] C. Pelekani, V.L. Snoeyink, Competitive adsorption between atrazine and methylene blue on activated carbon: The importance of pore distribution, Carbon 38 (2000) 1423–1436.